water

MDPI

Article

Groundwater Investigation through Electrical Resistivity Tomography in the Galhareri District, Galgaduud Region, Somalia: Insights into Hydrogeological Properties

Mahad Abdullahi Hussein [1,*], Mohammed Yusuf Ali [2] and Hassan Ali Hussein [3]

[1] Department of Geology, Faculty of Geosciences and Environment, Hormuud University, Mogadishu P.O. Box 046, Somalia
[2] Department of Earth Sciences, Khalifa University of Science and Technology, Abu Dhabi P.O. Box 127788, United Arab Emirates; mohammed.ali@ku.ac.ae
[3] Department of Geology, Faculty of Science, Somali National University, Mogadishu P.O. Box 15, Somalia; hhussein@snu.edu.so
* Correspondence: mahad@hu.edu.so or mahadsomali114@gmail.com

Abstract: Electrical resistivity tomography (ERT) was conducted to delineate groundwater potential zones in villages located in the Galhareri district of the Galgaduud region, central Somalia. A total of four ERT profiles were examined using the gradient configuration, chosen for its practical advantages over other configurations. The study revealed that all profiles were situated within similar geological environments, characterized by comparable rock types. However, notable disparities were observed in lithological variations, particularly in the texture of rocks encountered at different locations and in the thicknesses of the encountered geo-electric layers. The two-dimensional inversion results derived from the electrical resistivity data unveiled the presence of four geo-electrical layers. The first layer was interpreted as sand dunes. The second layer exhibited relatively higher resistivity values, indicating the presence of compact limestone and sandstone. The resistivity of the third layer suggested the existence of a lower resistivity layer, interpreted as weathered limestone, while the fourth layer demonstrated very low inverted resistivity, interpreted as sandy clay with sandstone. The ERT models constructed for the survey area effectively delineated the aquifer zone, represented by layer 3, which likely consists of weathered limestone, sandy clay, and sandstone. The resistivity values obtained for the aquifer zone, specifically at depths ranging from 200 to 300 m, were relatively low, suggesting that the groundwater quality is brackish in nature.

Keywords: aquifer; electrical resistivity tomography; groundwater; Galgaduud region; Somalia

Citation: Hussein, M.A.; Ali, M.Y.; Hussein, H.A. Groundwater Investigation through Electrical Resistivity Tomography in the Galhareri District, Galgaduud Region, Somalia: Insights into Hydrogeological Properties. *Water* **2023**, *15*, 3317. https://doi.org/10.3390/w15183317

Academic Editor: Kristine Walraevens

Received: 10 July 2023
Revised: 23 August 2023
Accepted: 8 September 2023
Published: 20 September 2023

1. Introduction

Somalia is recognized as one of the regions in the Horn of Africa that is highly susceptible to drought, with irregular and short-duration rainfall events [1]. The Galgaduud region, located in central Somalia, predominantly experiences an arid and semi-arid climate, rendering it particularly vulnerable to the risks of climate change-induced drought and water scarcity. The entire region has faced challenges associated with below-normal rainfall and limitations imposed by poor soil quality. Rainfall distribution follows a bi-modal pattern, characterized by isolated storms influenced by seasonal monsoon systems and shifts in monsoon winds. Central Somalia generally experiences two rainy seasons locally known as "Gu" (April to June) and "Deyr" (October to November), alternating with two dry seasons referred to as "Jilaal" (December to March) and "Haggaa" (July to September). Over the past five years, temperatures in the region have ranged from 21 °C to 40 °C, with an average temperature of 33 °C, contributing significantly to high rates of evapotranspiration. Consequently, the water supply situation in many parts of Somalia is critical, primarily due to the region's very low effective annual rainfall. As a result, groundwater development becomes a crucial water source in numerous areas. Despite various deep drilling projects undertaken in the Galgaduud region, the success rate of groundwater development and the drilling of productive wells has remained remarkably low, largely attributed to the lack of prior hydrogeological knowledge. Furthermore, studies have revealed poor groundwater quality in central Somalia, rendering it unsuitable for drinking purposes [2].

Geophysical surveys play a crucial role in the investigation of subsurface geologic phenomena and can provide valuable insights into surface geology. Within the realm of groundwater exploration, various geophysical techniques have been widely employed, including geo-electrical resistivity, electromagnetic (EM) profiling, seismic refraction, and geophysical borehole logging. Among these techniques, electrical resistivity methods have gained significant popularity in groundwater investigations [3–7]. Electrical resistivity techniques offer numerous advantages, such as their field-friendly nature, ability to provide subsurface information at depths ranging from a few meters to hundreds of meters, and the availability of software for 2D and 3D interpretation.

Moreover, the electrical resistivity method proves instrumental in addressing various hydrogeological challenges, including (1) monitoring industrial waste contamination and pollutants [8]); (2) determining the spatial extent of groundwater aquifers [9]); (3) estimating hydraulic parameters of aquifers [10,11]; (4) monitoring aquifer recharge [12]; and (5) and characterizing seawater intrusions in coastal groundwater aquifers [13,14]. Two geophysical methods are commonly employed to study the electrical resistivity characteristics of groundwater aquifers. EM methods offer the capability to detect shallow and deep groundwater aquifers [15], but they require costly equipment and necessitate precautions to avoid cultural and industrial noise as well as power lines. On the other hand, electrical methods encompass a range of techniques and configurations (arrays), making them suitable for noisy environments, and are the most prevalent techniques employed in hydrogeological investigations.

From 15 September to 20 September 2022, a 2D electrical resistivity tomography (ERT) survey was conducted in the Galhareri district of the Galgaduud region in central Somalia (Figure 1). The survey focused on three areas of interest, namely Haji Iiman, El Jiqow, and Daba-Duleel villages. The primary objectives of the survey were (a) to explore the groundwater aquifer and its electrical characteristics, (b) to gain insights into the resistivity structure and distribution beneath the survey area, and (c) to determine the depth and thickness of the aquifer and saturated zone, with the aim of facilitating future well-drilling endeavors for groundwater extraction.

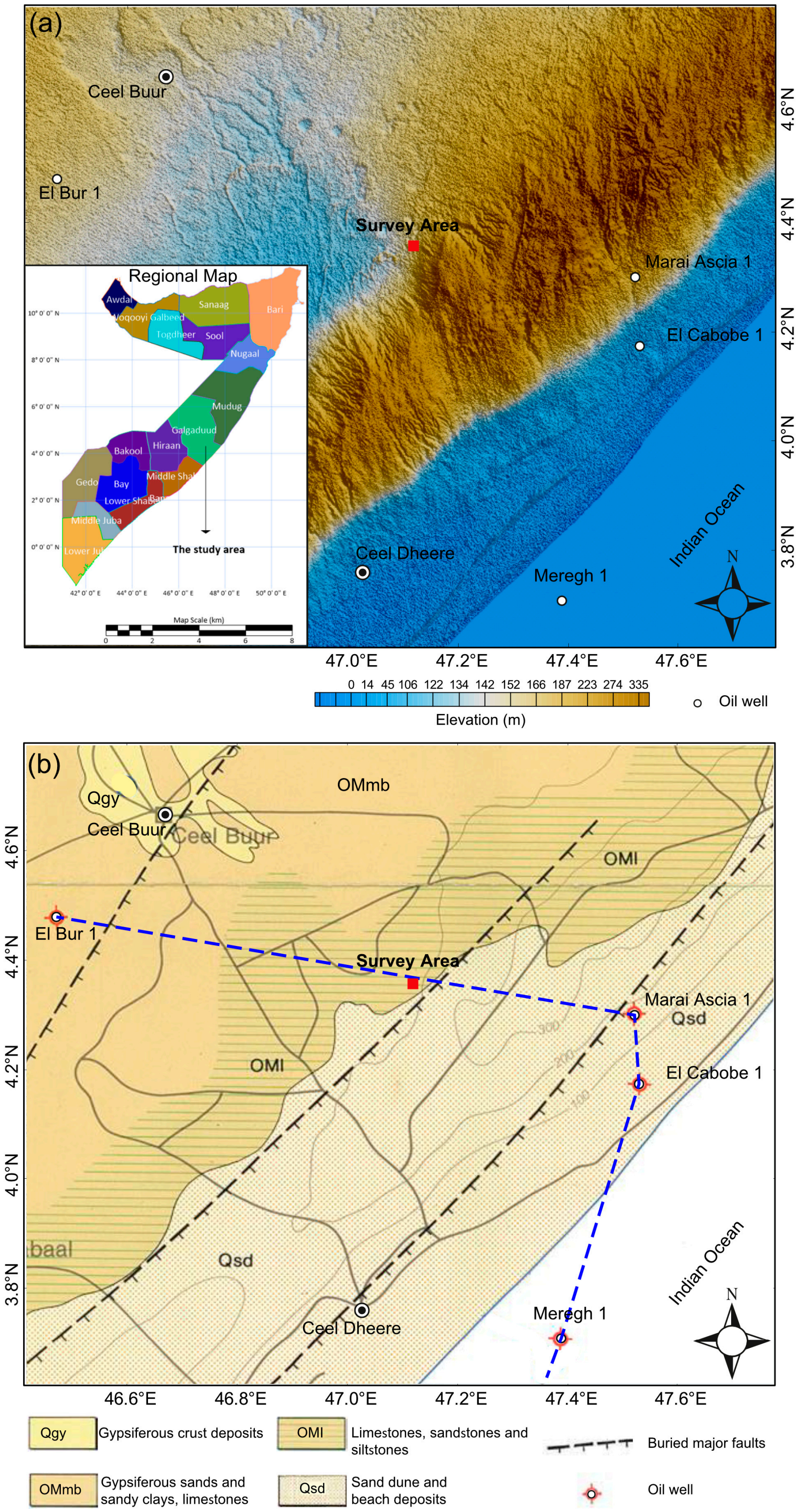

Figure 1. (**a**,**b**) Topographic and geological maps of the survey area. The locations of hydrocarbon exploration wells El Bur-1, Marai Ascia-1, El Cabobe-1, and Meregh-1 are also shown. The insert map shown in (**a**) displays the geographic map of Somalia. The red squares show the location of the survey area. The geology map is modified from [16]. The dashed blue line in (**b**) shows the location of the cross-section in Figure 2.

2. Geological Setting and Hydrogeology of the Survey Area

2.1. Geological Setting

The survey area is situated on the coastal plains of central Somalia, characterized by relatively flat terrain with elevations ranging from 200 to 350 m above sea level (Figure 1a). Numerous studies have been conducted to describe the geology of central Somalia, including works by [2,17]. Additionally, subsurface stratigraphy of the area has been derived from the drilling of four hydrocarbon exploration wells: El Bur-1, Marai Ascia-1, El Cabobe 1, and Meregh-1, with total depths (TDs) of 2621, 4115, 4428, and 4298 m, respectively (Figure 2).

The region exhibits a diverse range of sedimentary deposits spanning from the Miocene to Recent (Figure 1b). However, the predominant formations outcropping within the survey area consist of various continental Quaternary deposits, such as caliche and related rocks, secondary gypsum, gypsiferous clay, aeolian red sands, as well as Oligocene to Early Miocene deposits of the Mudug Succession, comprising gypsiferous sand, sandy clay, and limestones.

The hydrocarbon exploration wells drilled in the region penetrated thick Mesozoic (Adigrat to Yesomma formations) and Cenozoic (Auradu to Recent) sediments (Figure 2). The Upper Cretaceous Yesomma Formation predominantly comprises conglomerates, sandstones, sandy mudstones, and mudstones. Notably, the aquifer within the Yesomma Sandstone Formation is considered the most significant and primary water-bearing formation in Somalia.

The Eocene Auradu series, which follows the Yesomma Formation, consists of hard, massive limestone ranging in color from grey to white. The limestone often lacks bedding and is occasionally interbedded with thinly bedded layers of limestone, which may exhibit chalky and gypsiferous characteristics, along with calcareous shales. Another Eocene formation, the Taleh Formation, is widespread across central Somalia. This evaporitic formation, deposited under arid climatic conditions in a shallow sea environment, primarily consists of dense anhydrite beds, interspersed with layers of limestone and gypsum. Localized deposits of clay, sand, and gravel, transported by rivers in shallow lagoonal settings, can also be found within this sequence. Some areas exhibit lateral facies changes from gypsum and anhydrite to limestone, while changes from anhydrite to gypsiferous limestone and dense limestone are common and can be observed over relatively short distances.

During the upper Eocene and lower Oligocene, a shallow sea regression occurred, leading to the deposition of fossiliferous limestone and marls, forming the Karkar Formation. The Karkar Formation is characterized by bedded limestone, marly layers, and white marls. The limestone often exhibits karstification and possesses a well-developed system of caves. Thin layers of gypsum and occasional shale can also be encountered within certain sections of the formation. However, the Karkar Formation is totally eroded across central Somalia during the Miocene.

Throughout the Oligocene to Miocene period, the sea receded from central Somalia, giving rise to continental and lagoonal environments across most of the region. Thick layers of Pleistocene to Recent sediments were subsequently deposited within plateau areas, between foothills and coastal strips, as well as in valley fills and deltaic deposits. These sediments are seasonally transported by ephemeral streams during the rainy season. The superficial deposits primarily consist of quartz grains, ranging from fine to coarse. The grains exhibit a well-rounded shape and sorting, although they may be mixed with clay in some instances.

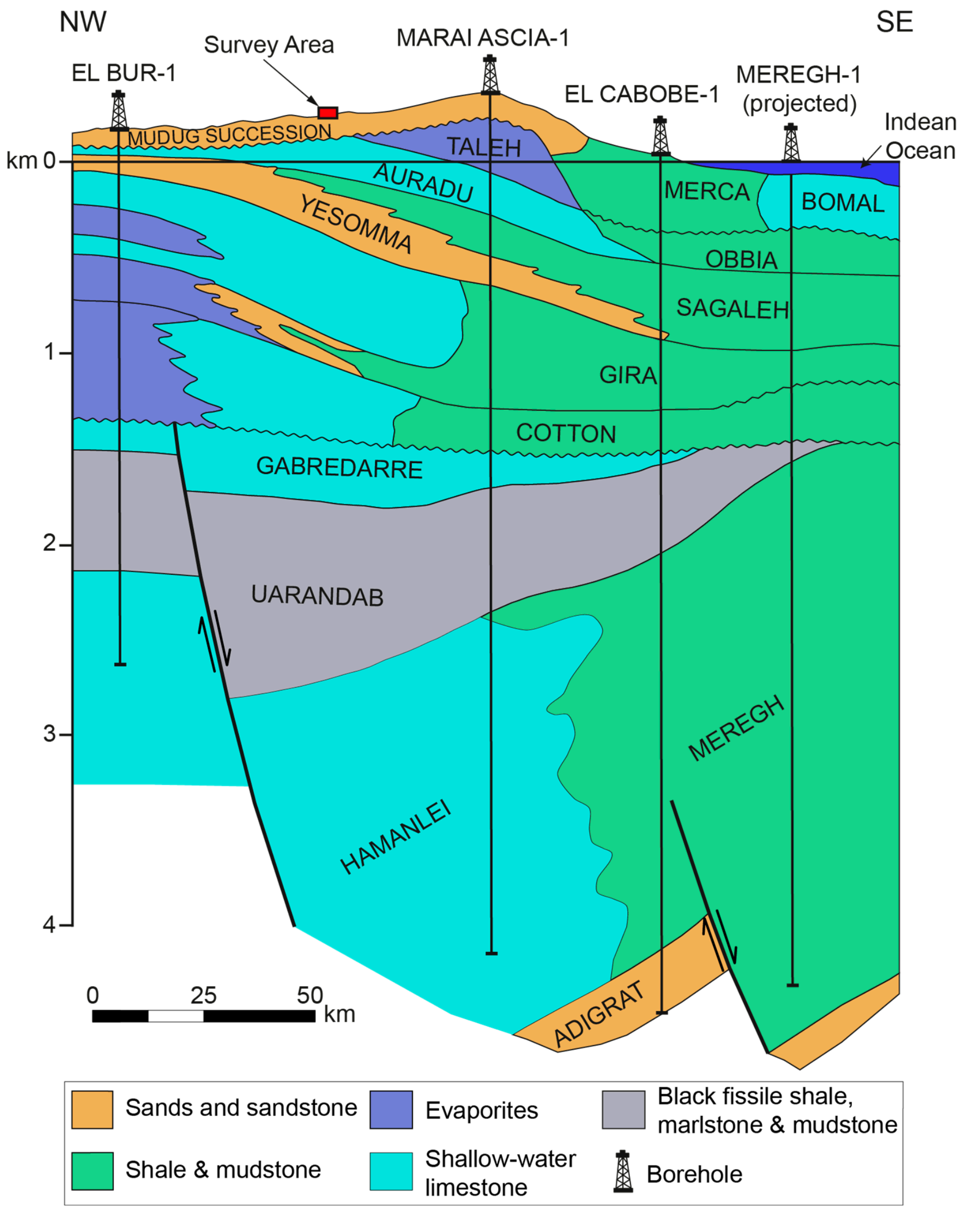

Figure 2. Correlation of hydrocarbon exploration wells (El Bur-1, Marai Ascia-1, El Cabobe-1, and Meregh-1) illustrating stratigraphy of the coastal plains of central Somalia. The survey area is highlighted in the red box. Refer to Figure 1 for the location of the profile. The figure is modified from [18].

2.2. Hydrogeology of the Survey Area

A comprehensive understanding of the hydrogeological conditions in the survey area, including groundwater flow patterns, electrical properties, and other hydrogeological characteristics, can be attained through a thorough knowledge of the stratigraphy and geological structures.

Surface water resources in the survey area are limited. There are no perennial rivers, except for small seasonal Wadis or streams that temporarily flow during the rainy seasons (Gu and Deyr seasons) for short durations. These watercourses are mostly ephemeral and originate from the Ogaden plateau in Ethiopia, flowing towards the east. However, surface water availability is practically nonexistent as the rainfall in the catchment areas is largely lost through evaporation and infiltration.

Groundwater serves as the primary water source in the survey area, with two main types of groundwater resources: shallow wells and deep boreholes. The shallow aquifers, accessed through hand-dug wells, are located within a broad depression covered by gypsiferous soils, gypsum, and limestone, often following the ancestral drainage systems. The depths and water table levels of shallow aquifers vary across different locations, with water depths generally exceeding 15 m and water table depths ranging between 4 and 6 m.

There are no boreholes drilled within the survey area. However, based on borehole lithological logs in the surrounding areas, groundwater aquifers are encountered within sandstone, porous limestone, and white marl. Drilled boreholes suggest that aquifers generally occur at depths ranging from 70 m to over 200 m below the ground level (Table 1). The aquifer zones within the shallow marine limestone formations are semi-confined to confined, with reported yields ranging from 12 m^3/h to 22 m^3/h in boreholes penetrating these formations. Available data on electrical conductivity (EC) values for boreholes ranging from 180 to 304 m in depth indicate values between 3000 µS/cm and 8000 µS/cm, with total dissolved solids (TDSs) ranging from 2000 to 5000 ppm. These results suggest that water quality in the survey area is poor, primarily due to higher salinity resulting from the chemical composition of the surrounding rocks. Boreholes drilled in surrounding areas (e.g., Bida Ciise, Ceel Jiqow and Baraag Shador, Table 1) were used to verify and improve the accuracy of electrical resistivity tomography results.

Table 1. Water boreholes drilled in the surrounding area of the survey area.

Borehole Name	Total Depth (m)	Distance from Study Area (km)	Lithology
Bida Ciise	270	45	0–10 m: Recent sands 10–100 m: Quaternary deposits consisting of sand clay, sand and sandstone 100–180 m: Mudug Succession consisting of sandstone aquifer with EC of 3000 µS/cm 180–270 m: Auradu Formation consisting of weathered limestone aquifer with EC of 4000 to 8000 µS/cm
Ceel Jiqow	80	10	0–20 m: Recent sands 20–35 m: Quaternary deposits consisting of sandy clay 35–80 m: Mudug Succession consisting of sandstone aquifer with EC of 4000 µS/cm
Baraag Shador	304	25	0–16 m: Recent sands 16–120 m: Quaternary deposits consisting of sand clay, sand and sandstone 120–189 m: Mudug Succession consisting of sandstone aquifer with EC of 3000 µS/cm 189–304 m: Auradu Formation consisting of weathered limestone aquifer with EC of 4000 to 8000 µS/cm

3. Methodology and Data

Electrical Resistivity Tomography (ERT) represents a widely employed geo-electric method aimed at generating 2D or 3D images that exhibit high-resolution variability in the electrical resistivity of geological media. ERT measurements exhibit sensitivity to subsurface material properties, including electrolyte characteristics, porosity, water saturation, and salinity [19,20]. This technique has found extensive utility in the exploration of aquifer resources and environmental engineering inquiries [21–24]. The technique is founded upon the assessment of apparent resistivity distribution and alterations in the artificially induced electric field facilitated by an array of electrodes. Noteworthy attributes of ERT encompass its efficient survey capabilities, substantial data output, a wealth of information, precise observational acuity, and rapid execution. Consequently, it stands out as one of the most efficacious geophysical approaches for detecting structural fractures and zones of heightened groundwater presence.

The ERT methodology operates in accordance with Ohm's law, as represented by Equation (1):

$$\Delta V = IR \quad (1)$$

This involves the utilization of paired current electrodes for the injection of current (I) into the subsurface and potential electrodes for the measurement of potential difference (ΔV) between arbitrary points within a predetermined distance.

Electrical resistivity (ρ) serves as a quantification of resistance (R, calculated as $\Delta V = I$ across a cross-sectional area (A) involving a wire of length (l)). It is defined by Equation (2):

$$\rho = RA/l \quad (2)$$

Within ERT, the apparent resistivity (ρa) can be derived by employing Equation (3):

$$\rho a = K\Delta V/I \quad (3)$$

here K signifies a geometric factor intrinsic to the layouts of the current and potential electrodes.

In September 2022, a total of four ERT profiles were acquired to comprehensively investigate the hydrogeological strata within the survey area. These profiles were strategically collected in the proximity of Haji Iiman and El Jiqow and Daba Duleel villages (Figure 3). The employment of ERT facilitated the creation of subsurface sections, enabling the deduction of insights concerning the distribution and thicknesses of aquifer zones [19]. The execution of ERT encompassed the utilization of the ABEM Terrameter LS 2 multi-electrode resistivity imaging system, coupled with supplementary tools including a Garmin GPS device, compass, and roll-up tape measure.

The ABEM Terrameter LS 2 instrument, globally renowned for its proficiency in resistivity and IP imaging, was harnessed to chart and ascertain the resistivity values of underlying lithological formations. This endeavor aimed to evaluate their potential as aquifers and to estimate groundwater quality. The system's configuration incorporates four sets of multi-core cables, each furnished with 16 electrodes. This arrangement facilitates automated switching of measurements across diverse pairs of current and potential electrodes, systematically positioned at equidistant intervals along pre-established survey lines.

The electrode spacing was consistently maintained at 20 m throughout the survey, with variations in length and orientation. The maximum distances between current dipoles and electrodes were determined as follows: 1620 m, 1620 m, 2000 m, and 1200 m for Profiles 1, 2, 3, and 4, respectively. The gradient protocol, chosen for its sensitivity to vertical and lateral geological structures as well as its high horizontal and vertical resolutions, was applied across all survey sites. A thorough electrode test was conducted to verify the performance and ensure good ground contact for each electrode. For electrodes with poor contact, a salt solution was applied to reduce contact resistance. The measurement sequence was completed within a timeframe of 30 to 40 min. During data acquisition, the four basic electrodes could be either active or passive, as they were selected simultaneously.

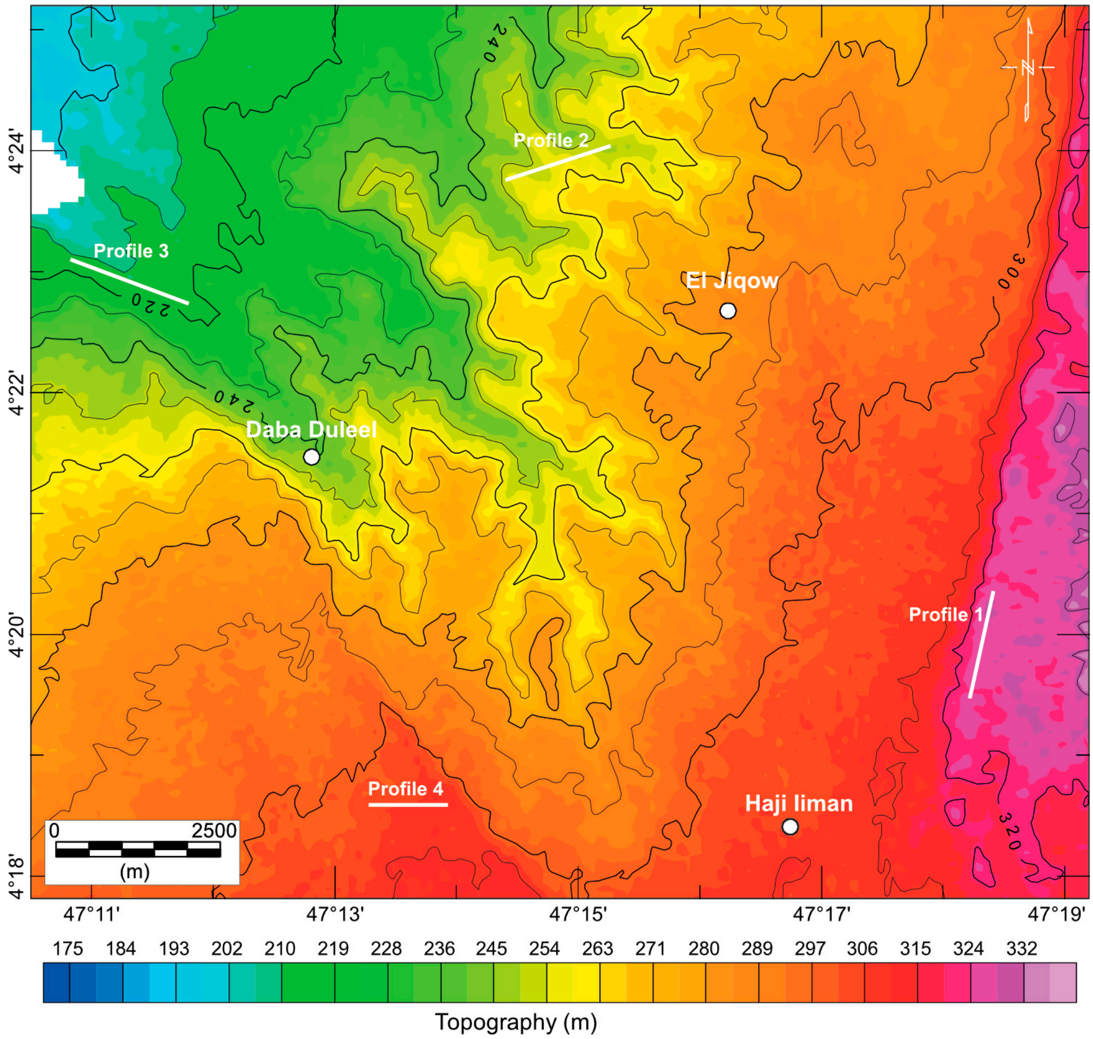

Figure 3. Shuttle radar topography map of the survey area showing locations of the villages and ERT profiles. Spacing between contour lines is 10 m. Refer to Figure 1 for the location of the survey area. The ERT profiles were acquired on a relatively flat topography.

In the processing of the ERT data, the initial step involved the removal of noisy data points from each ERT line. These noisy values, characterized by negative and excessively high resistivity, were attributed to high contact resistance at specific electrode locations. Despite the use of salty water to reduce contact resistance, some electrodes exhibited noisy data due to the challenging surface geology consisting of dry gravel and sand materials. Nevertheless, the overall data quality is very good. The similarity among the four profiles of the four pseudosections indicates good quality signals were measured (Figures 4–7). After editing each ERT dataset to eliminate the noisy values, the apparent resistivity values were inverted to obtain the true resistivity values along the survey lines.

The processing procedures applied to the field data encompassed several pivotal stages, namely data reading and format conversion, elimination of erroneous data points, topographic correction, determination of inversion parameters, actual inversion, and final cartographic representation. For the manipulation of apparent resistivity measurements, the Res2DInv inversion software version 4.10, developed by Aarhus GeoSoftware, Aarhus, Denmark, was employed. This software package stands as a preeminent choice for ERT data processing, widely acknowledged for its extensive usage. It effectively generates a 2D resistivity inversion section that vividly delineates variations in the electrical characteristics of subsurface features. The Res2DInv software employs a finite-difference modeling subroutine to calculate the real resistivity values, while a non-linear smoothness-constrained least-squares optimization technique is used to calculate the resistivity of the model blocks [25,26]). One advantage of this method is its ability to adjust the damping factor and roughness filters to reduce large horizontal and vertical resistivity differences, so the obtained model parameters do not change abruptly. Beginning with an initial model, typically a homogeneous earth model, the program calculates the change in model parameters that minimize the difference between the calculated and measured apparent resistivity values [20]. It adjusts the resistivity of the model blocks while adhering to the imposed smoothness constraints. The root-mean-squared (RMS) error measures the difference between the calculated and measured values. However, the model with the lowest RMS error may exhibit large and unrealistic variations in the resistivity values, and may not always be the most geologically plausible model. As a general practice, it is prudent to select the model at the iteration where the RMS error stabilizes and no longer changes significantly, typically occurring between the 3rd and 6th iterations. The resulting output model provides a section that shows resistivity distribution beneath the profile. This distribution must be interpreted based on available subsurface information. In case no data are available, the uncertainty in the interpretation should be expressed.

4. Results and Discussion

Figures 4–7 show the measured apparent resistivity psedusections, calculated apparent resistivity psedusections, and inverse model resistivity sections of the four profiles. The results obtained from the inversion of the ERT data provide valuable and detailed insights into the hydrogeological properties of the aquifer system within the surveyed area (see Figures 4c, 5c, 6c and 7c). The inverted ERT sections reveal significant lateral and vertical variations in true resistivity, unveiling the presence of four distinct layers with unique characteristics.

The ERT results consistently demonstrate the existence of four geo-electrical layers throughout the survey area. The resistivity values observed in the ERT profiles exhibit a considerable range, spanning from 0.5 to 105 Ωm, indicating a wide variability in subsurface lithology. The depth penetration achieved by the ERT measurements extends to approximately 282 to 435 m below the ground surface (23 m above sea level to −220 m below sea level), offering valuable insights into the deeper layers of the subsurface (see Figures 4–7)).

The analysis of the ERT data enabled the identification and characterization of different geo-electrical layers, each exhibiting its own unique resistivity range and thickness. Through a comprehensive interpretation process, informed by local geological knowledge and the integration of available drilling logs from the surrounding areas, the individual sections of the resistivity model were examined and correlated with the underlying geological formations.

The first layer observed in the resistivity model, characterized by resistivity values ranging from 15 to 20 Ωm and a thickness of approximately 30 to 40 m, can be confidently interpreted as the sand dune layer and silty sand sediments as documented on the surface geology of the survey area and nearby boreholes (Table 1). This layer represents the near-surface deposits consisting of loose, unconsolidated sand, and it plays a crucial role in controlling surface water infiltration and recharge processes.

The second layer, distinguished by relatively higher resistivity values ranging from 60 to 100 Ωm, points to the presence of compact limestone and sandstone formations. This layer is characterized by its significant thickness variations, ranging from 30 to 50 m in Profiles 1 to 3 (Figures 4c, 5c, 6c and 7c), and exhibiting a remarkable thickness extension of up to 200 m in Profile 4 (see Figure 7c). The variations in lithology and thickness within this layer suggest the presence of geological structures and sedimentary facies changes that contribute to the heterogeneity of the aquifer system. This layer is potentially attributed to the Mududg Succession, as indicated in Table 1.

The resistivity values of the third layer indicate the presence of a lower resistivity zone, typically ranging from 10 to 20 Ωm. The resistivity values of this layer are compatible with marl or marly limestone. However, we interpreted it as weathered limestone, suggesting a zone of altered and fractured rock material that has undergone chemical weathering processes over time. The weathered limestone layer often exhibits enhanced porosity and permeability, which can significantly influence groundwater flow and storage characteristics. This is consistent with the finding of the Bida Ciise and Baraag Shador boreholes (Table 1), which penetrated a weathered limestone within the Auradu Formation with EC values of 4000 to 8000 µS/cm at a depth of 180–270 m below the surface.

Lastly, the fourth layer, displaying very low inverted resistivity values below 10 Ωm, is interpreted as sandy clay interbedded with sandstone. This layer represents fine-grained sediments with limited hydraulic conductivity, potentially acting as an aquitard or confining layer that impedes vertical groundwater movement between the upper aquifer zones and the deeper geological formations. This layer can also represent deeper Auradu limestone saturated with brackish water.

The comprehensive analysis of the ERT models and geological information reveals crucial information about the aquifer system in the survey area. The total depth captured by the ERT sections extends approximately from 220 to 420 m, providing valuable insights into the deeper geological formations and their hydrogeological properties. Notably, the ERT models have successfully delineated an aquifer zone with a thickness ranging from approximately 100 to 130 m and a top depth varying from 150 to 200 m (see Figures 4c, 5c, 6c and 7c). This aquifer zone consists of weathered limestone, sandy clay, and sandstone, suggesting the presence of potential groundwater resources. However, it is important to note that the resistivity values observed in the aquifer zone are relatively low, implying the presence of brackish water with higher salinity levels.

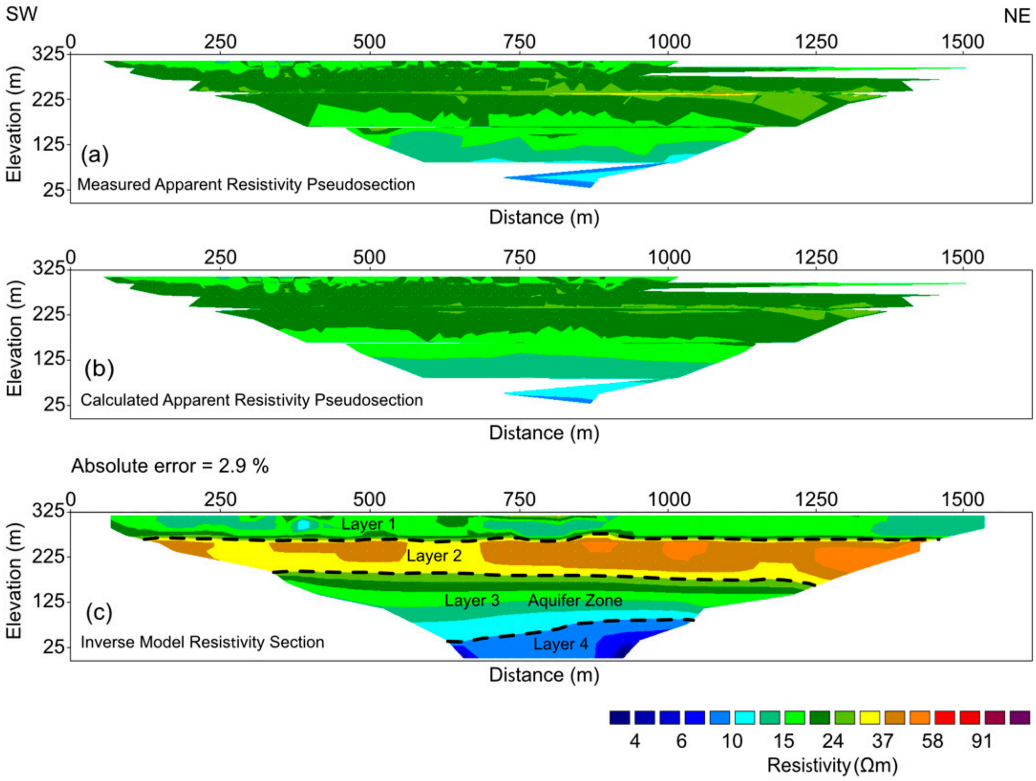

Figure 4. (**a**) Measured apparent resistivity pseudosection, (**b**) calculated apparent resistivity pseudosection, and (**c**) inverted section of Profile 1 showing interpreted hydrogeological layers on the basis of borehole data and surface geology of the area. The RMS is 2.9%. The vertical axis is the elevation above sea level. Refer to Figure 3 for the location of the profile.

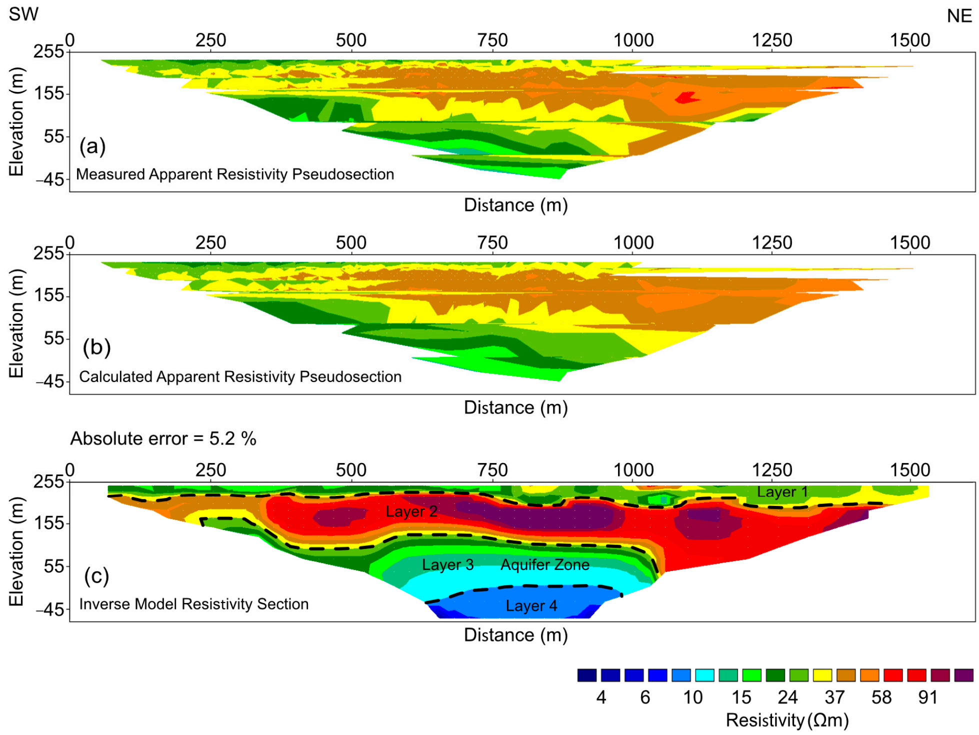

Figure 5. (**a**) Measured apparent resistivity pseudosection, (**b**) calculated apparent resistivity pseudosection, and (**c**) inverted section of Profile 2 showing interpreted hydrogeological layers on the basis of borehole data and surface geology of the area. The RMS is 5.2%. Refer to Figure 3 for the location of the profile.

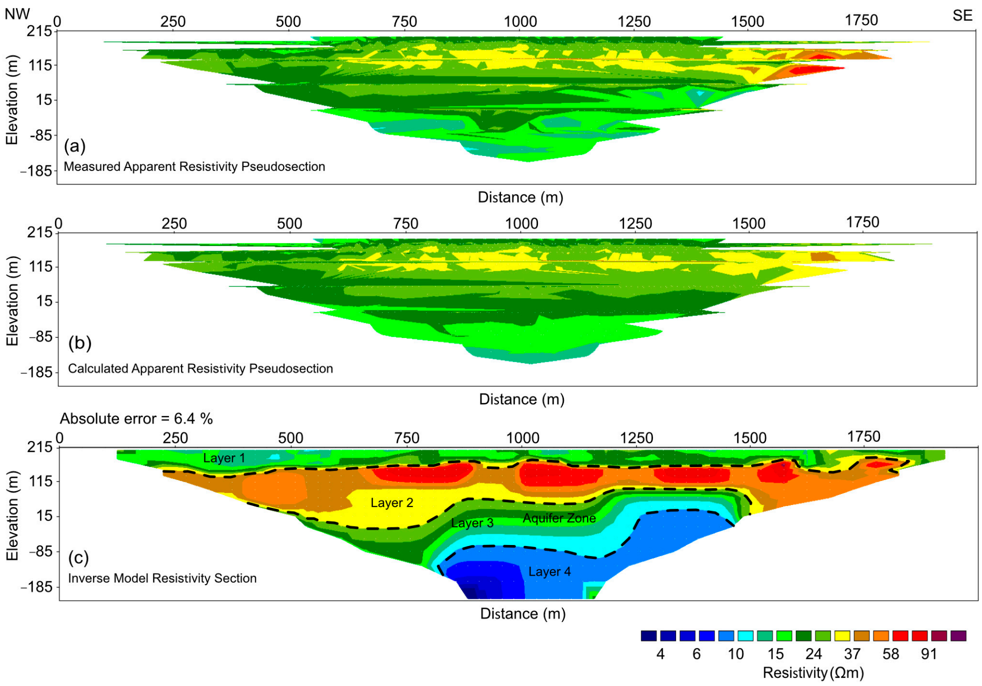

Figure 6. (**a**) Measured apparent resistivity pseudosection, (**b**) calculated apparent resistivity pseudosection, and (**c**) inverted section of Profile 3 showing interpreted hydrogeological layers on the basis of borehole data and surface geology of the area. The RMS is 6.4%. Refer to Figure 3 for the location of the profile.

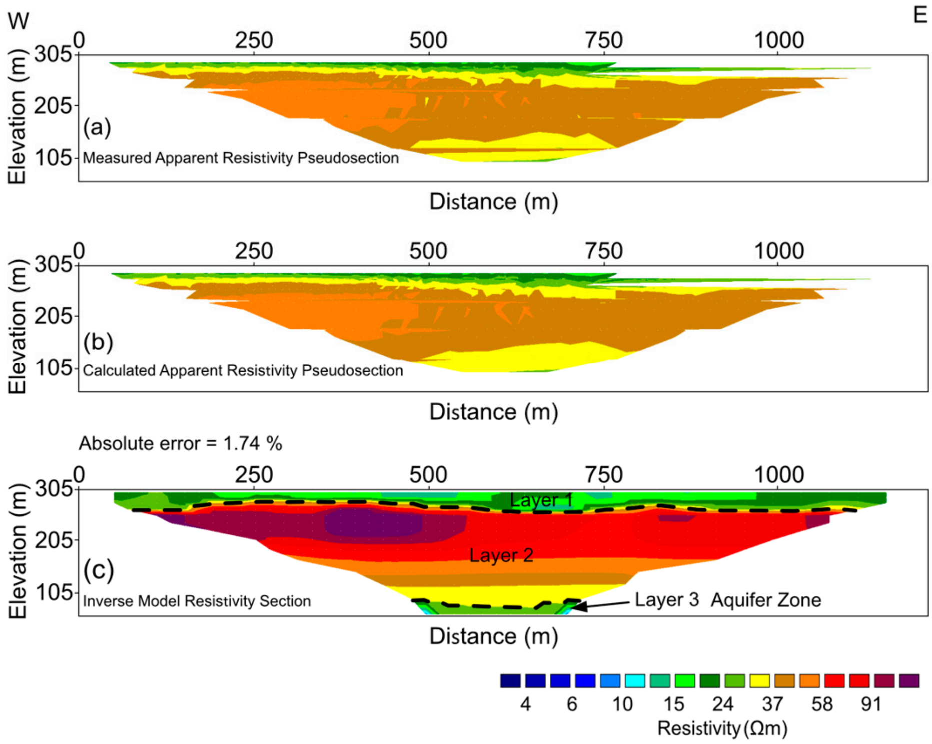

Figure 7. (**a**) Measured apparent resistivity pseudosection, (**b**) calculated apparent resistivity pseudosection, and (**c**) inverted section of Profile 4 showing interpreted hydrogeological layers on the basis of borehole data and surface geology of the area. The RMS is 1.74%. Refer to Figure 3 for the location of the profile.

5. Conclusions

This study utilized ERT to assess groundwater potential zones in villages located in the Galhareri district of the Galgaduud region, central Somalia. The investigation involved the examination of four ERT profiles using the gradient configuration, which offered practical advantages for this study. The geological environments in all profiles were found to be similar, characterized by comparable rock types. However, variations in lithology, particularly in rock texture and layer thickness, were observed across different locations.

The two-dimensional inversion of the electrical resistivity data revealed the presence of four distinct geo-electrical layers. The first layer was identified as sand dunes, while the second layer exhibited higher resistivity values indicative of compact limestone and sandstone. The third layer displayed lower resistivity, suggesting the presence of weathered limestone. Lastly, the fourth layer exhibited very low resistivity, indicating sandy clay with sandstone.

The constructed ERT models effectively delineated the aquifer zone, represented by layer 3, which is likely composed of weathered limestone, sandy clay, and sandstone. The resistivity values obtained within this aquifer zone, particularly at depths ranging from 200 to 300 m, were relatively low, indicating a brackish nature of the groundwater.

These findings provide valuable insights into the hydrogeological characteristics of the study area. It is evident that the groundwater potential in the surveyed villages is influenced by the geological composition and layer variations. The delineation of the aquifer zone and the determination of its properties through ERT profiling contribute to a better understanding of the groundwater resources in the region.

Based on the results, it can be concluded that the study area exhibits moderate to poor groundwater potential. The aquifer is located at depths exceeding 200 m below the ground level and is characterized by brackish water quality. This information is crucial for local water resource management and can aid in the development of appropriate strategies for sustainable groundwater utilization in the Galhareri district of the Galgaduud region, central Somalia. Further investigations and monitoring, including Time Domain electromagnetic methods, are recommended to enhance our understanding of the aquifer dynamics, increase the depth of investigation, and guide future water resource planning and management efforts in the area.

Author Contributions: Conceptualization, M.A.H.; methodology, M.A.H. and M.Y.A.; software, M.A.H. and M.Y.A.; validation, M.A.H., M.Y.A. and H.A.H.; formal analysis, M.A.H. and M.Y.A.; investigation, M.A.H. and M.Y.A.; resources, M.A.H. and M.Y.A.; data curation, M.A.H. and M.Y.A.; writing—original draft preparation, M.A.H. and M.Y.A.; writing—review and editing, M.A.H., M.Y.A. and H.A.H.; visualization, M.A.H. and M.Y.A.; supervision, M.Y.A. and H.A.H.; project administration, M.A.H.; funding acquisition, M.A.H. All authors have read and agreed to the published version of the manuscript.

Funding: The article was funded by Hormuud University, Mogadishu, Somalia.

Data Availability Statement: Data are contained within the article.

Acknowledgments: The authors would like to thank all of their colleagues who helped with this research. We are grateful to the local community and elders in Galhareri for their generosity and support of us during this difficult work. We thank Hormuud University for supporting this study by providing equipment and logistics.

Conflicts of Interest: The authors declare no conflict of interest.

References

1. FAO-SWALIM. *Hydrogeological Survey and Assessment of Seletced Areas in Somaliland and Puntland*; Technical Report No. W-20; FAO-SWALIM (GCP/SOM/049/EC) Project: Nairobi, Kenya, 2012.
2. Faillace, C.; Faillace, E.R. *Water Quality Data Book of Somalia: Hydrogeology and Water Quality of South Central Somalia*; Deutsche Gesellschaft für Internationale Zusammenarbeit (GIZ): Rome, Italy, 1986; Volume 1.
3. El-Qady, G.; Ushijima, K. Inversion of DC resistivity data using neural networks. *Geophys. Prospect.* **2001**, *49*, 417–430. [CrossRef]
4. Ghosh, D.P. The application of linear filter theory to the direct interpretation of geoelectrical resistivity sounding measurements. *Geophys. Prospect.* **1971**, *19*, 192–217. [CrossRef]
5. Griffith, D.H.; Rooney, W.J. Two-dimensional resistivity imaging and modeling in areas of complex geology. *J. Appl. Geophys.* **1993**, *29*, 211–226. [CrossRef]
6. Loke, M.H.; Dahlin, T.; Rucker, D.F. Recent developments of the direct-current geoelectrical imaging method. *Geophysics* **2014**, *95*, 135–156. [CrossRef]
7. Telford, W.M.; Geldart, L.P.; Sheriff, R.E. *Applied Geophysics*, 2nd ed.; Cambridge University Press: Cambridge, UK, 1990.
8. Rockhold, M.L.; Robinson, J.L.; Parajuli, K.; Song, X.; Zhang, Z.F.; Johnson, T.C. Groundwater characterization and monitoring at a complex industrial waste site using electrical resistivity imaging. *Hydrogeol. J.* **2020**, *28*, 2115–2127. [CrossRef]
9. Greggio, N.; Giambastiani, B.M.S.; Balugani, E.; Amaini, C.; Antonellini, M. High-Resolution Electrical Resistivity Tomography (ERT) to Characterize the Spatial Extension of Freshwater Lenses in a Salinized Coastal Aquifer. *Water* **2018**, *10*, 1067. [CrossRef]
10. De Clercq, T.; Jardani, A.; Fischer, P.; Thanberger, L.; Vu, T.M.; Pitaval, D.; Côme, J.-M.; Begassat, P. The use of electrical re-sistivity tomograms as a parameterization for the hydraulic characterization of a contaminated aquifer. *J. Hydrol.* **2020**, *587*, 124986. [CrossRef]
11. Kazakis, N.; Vargemezis, G.; Voudouris, K. Estimation of hydraulic parameters in a complex porous aquifer system using geoelectrical methods. *Sci. Total. Environ.* **2016**, *550*, 742–750. [CrossRef] [PubMed]
12. Sendrós, A.; Himi, M.; Lovera, R.; Rivero, L.; Garcia-Artigas, R.; Urruela, A.; Casas, A. Electrical resistivity tomography monitoring of two managed aquifer recharge ponds in the alluvial aquifer of the Llobregat River (Barcelona, Spain). *Near Surf. Geophys.* **2020**, *18*, 353–368. [CrossRef]
13. Galazoulas, E.C.; Mertzanides, Y.C.; Petalas, C.P.; Kargiotis, E.K. Large Scale Electrical Resistivity Tomography Survey Correlated to Hydrogeological Data for Mapping Groundwater Salinization: A Case Study from a Multilayered Coastal Aquifer in Rhodope, Northeastern Greece. *Environ. Process.* **2015**, *2*, 19–35. [CrossRef]
14. Niculescu, B.M.; Andrei, G. Application of electrical resistivity tomography for imaging seawater intrusion in a coastal aquifer. *Acta Geophys.* **2021**, *69*, 613–630. [CrossRef]
15. McNeill, J.D. Use of Electromagnetic Methods for Groundwater Studies. In *Geotechnical an Environmental Geophysics: Volume I: Review and Tutorial*; Society of Exploration Geophysicists: Houston, TX, USA, 1990; pp. 191–218. [CrossRef]
16. Abbate, E.; Sagri, M.; Sassi, F.P. *The Geological Map of Somalia 1:1.500*; University of Florence: Florence, Italy, 1994.
17. Muthusi, F.M.; Mugo, M.W.; Gadain, H.M. *Water Sources Inventory for Central—South Somalia*; Technical Report No W-17; FAO-SWALIM (GCP/SOM/048/EC) Project: Nairobi, Kenya, 2009.

18. Bosellini, A. *The Continental Margins of Somalia: Structural Evolution and Sequence Stratigraphy: Chapter 11: African and Mediterranean Margins*; Istituto di geologia e mineralogia, Universita di Padova: Padova, Italy, 1992.
19. Oldenborger, G.A.; Knoll, M.D.; Routh, P.S.; LaBrecque, D.J. Timelapse ERT monitoring of an injection/withdrawal experiment in a shallow unconfined aquifer. *Geophysics* **2007**, *72*, F177–F187. [CrossRef]
20. Chiang, C.W.; Hsu, H.L.; Chen, C.C. An investigation of the 3D electrical resistivity structure in the Chingshui geothermal area, NE Taiwan. *Terr. Atmos. Ocean. Sci.* **2015**, *26*, 269–281. [CrossRef]
21. Daily, W.; Ramirez, A.; Labrecque, D.; Nitao, J. Electrical resistivity tomography of vadose water movement. *Water Resour. Res.* **1992**, *28*, 1429–1442. [CrossRef]
22. Zhang, G.; Lü, Q.-T.; Zhang, G.-B.; Lin, P.-R.; Jia, Z.-Y.; Suo, K. Joint Interpretation of Geological, Magnetic, AMT, and ERT Data for Mineral Exploration in the Northeast of Inner Mongolia, China. *Pure Appl. Geophys.* **2018**, *175*, 989–1002. [CrossRef]
23. Loke, M.H. Electrical Imaging Surveys for Environmental and Engineering Studies: A Practical Guide to 2-D and 3-D Surveys. 2000, p. 61. Available online: https://pages.mtu.edu/~ctyoung/LOKENOTE.PDF (accessed on 1 July 2023).
24. Tsai, W.-N.; Chen, C.-C.; Chiang, C.-W.; Chen, P.-Y.; Kuo, C.-Y.; Wang, K.-L.; Lin, M.-L.; Chen, R.-F. Electrical Resistivity Tomography (ERT) Monitoring for Landslides: Case Study in the Lantai Area, Yilan Taiping Mountain, Northeast Taiwan. *Front. Earth Sci.* **2021**, *9*, 737271. Available online: https://www.frontiersin.org/articles/10.3389/feart.2021.737271 (accessed on 1 July 2023). [CrossRef]
25. Loke, M. Tutorial: 2-D and 3-D Electrical Imaging Surveys. Penang, Malaysia, University of Sains Malaysia. Unpublished Course Notes. 2001. Available online: http://personales.upv.es/jpadin/coursenotes.pdf (accessed on 1 July 2023).
26. Graziani, C.; Duranti, A.; Morelli, A.; Busani, L.; Pezzotti, P. Zoonosi in Italia nel Periodo 2009-Rapporti ISTISAN. Available online: http://www.epicentro.iss.it/ben/2010/gennaio/1.asp (accessed on 1 July 2023).